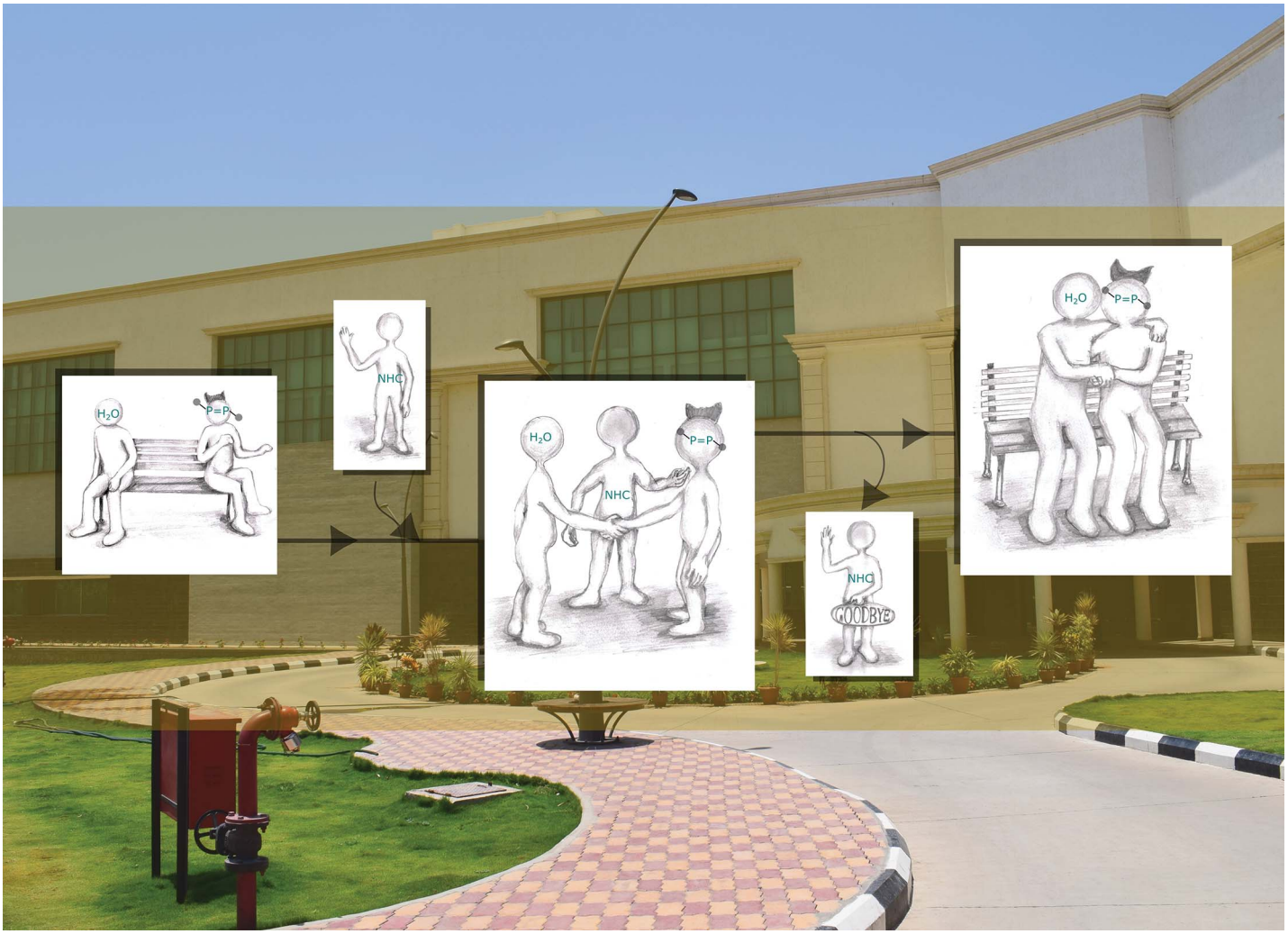

Showcasing research from Dr Anukul Jana's laboratory, Tata Institute of Fundamental Research, Hyderabad, India, along with collaboration between Professor V. Chandrasekhar, TIFR Hyderabad, India and Professor Dr David Scheschkewitz, Saarland University, Germany

Reactivity enhancement of a diphosphene by reversible N-heterocyclic carbene coordination

This paper is dedicated to Professor G. Mehta on his 75th birthday.

We have demonstrated the reversible coordination of N-heterocyclic carbene (NHC), a Lewis base, to a diphosphene, which leads to the reactivity enhancement of the diphosphene moiety, resulting in a ready hydrolysis and hydrogenation reaction. We were able to show that the hydrolysis reaction is catalytic.

As featured in:

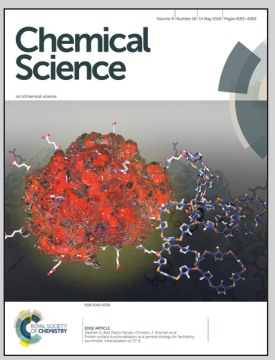

See Cem B. Yildiz, David Scheschkewitz, Vadapalli Chandrasekhar, Anukul Jana *et al.*, *Chem. Sci.*, 2018, **9**, 4235.

ROYAL SOCIETY OF CHEMISTRY

rsc.li/chemical-science

Registered charity number: 207890

Chemical Science

EDGE ARTICLE

View Article Online
View Journal | View Issue

Cite this: *Chem. Sci.*, 2018, **9**, 4235

Reactivity enhancement of a diphosphene by reversible N-heterocyclic carbene coordination†

Debabrata Dhara, [a] Pankaj Kalita, [b] Subhadip Mondal,[a] Ramakirushnan Suriya Narayanan, [a] Kaustubh R. Mote, [a] Volker Huch,[c] Michael Zimmer,[c] Cem B. Yildiz, *[d] David Scheschkewitz, *[c] Vadapalli Chandrasekhar *[ae] and Anukul Jana *[a]

Received 22nd January 2018
Accepted 26th March 2018

DOI: 10.1039/c8sc00348c

rsc.li/chemical-science

Diphosphene $Ter^{Mes}P=PTer^{Mes}$ (**1**; Ter^{Mes} = 2,6-$Mes_2C_6H_3$; Mes = 2,4,6-$Me_3C_6H_2$) and NHC^{Me_4} **2** (NHC^{Me_4} = 1,3,4,5-tetramethylimidazol-2-ylidene) exist in an equilibrium mixture with the NHC^{Me_4}-coordinated diphosphene **3**. While uncoordinated **1** is inert to hydrolysis, the NHC adduct **3** readily undergoes hydrolysis to afford a phosphino-substituted phosphine oxide with the liberation of NHC^{Me_4}. On this basis, conditions suitable for the catalytic use of NHC^{Me_4} were identified. Similarly, while the hydrogenation of free diphosphene **1** with $H_3N{\cdot}BH_3$ is very slow, **3** reacts instantaneously with $H_3N{\cdot}BH_3$ at room temperature to afford a dihydrodiphosphane.

Introduction

Reversible coordination/binding between the substrate and catalyst is pivotal to catalytic reactions. This paradigm has been the raison d'être for the use of a vast number of transition metal complexes in catalysis as exemplified by many celebrated compounds such as Wilkinson's catalyst.[1] Another crucial feature of many catalytic reactions is the role of auxiliary Lewis bases/donors in the activation of the catalyst to facilitate product formation.[2] While transition metal complexes are a strong mainstay in this field, there have been efforts to examine if systems based on main-group elements can also be useful in catalytic reactions. An important challenge in this endeavor is the design of compounds that, like their transition metal counter parts, are involved in reversible reactions with substrates and auxiliary activators such as bases.[3] An important breakthrough in this area has been the seminal report of Stephan and co-workers on the reversible activation of dihydrogen by the frustrated Lewis pair effect of a compound containing a P–B motif.[4] Numerous other reports followed including the reversible coordination/binding of ethylene with distannynes,[5] phosphines with CO_2,[6] N-heterocyclic carbenes with cyclotrisilenes,[7] and reversible oxidative addition of organoboronate esters at the carbon(II) center of cyclic alkyl amino carbene.[8] Main-group compounds can indeed display a transition metal-like behavior as exemplified by the stoichiometric activation of small molecules[9] as well as ligand exchange at the reactive low-valent centers.[10]

In the above context, recently Bertrand *et al.* reported a singlet (phosphino)phosphinidene, **I**, which is electrophilic despite its P–P multiple bond character and the presence of a formal negative charge at the phosphinidene center.[11] It was also shown that ligand exchange could occur at the phosphinidene centre of **I** (Scheme 1).[12] On the other hand, Robinson's NHC^{Dip}-stabilized P_2, **II** (Scheme 1)[13] which can be considered as an interconnected bis-phosphinidene dimer does not undergo ligand exchange with more nucleophilic NHCs such as NHC^{Me_4} and $NHC^{iPr_2Me_2}$.[14]

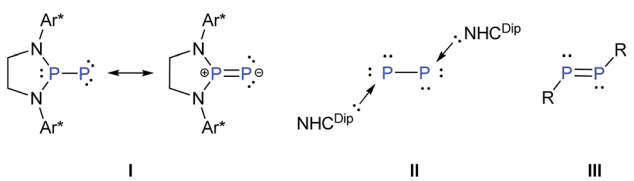

I II III

Scheme 1 Chemical structures of phosphino phosphinidene **I**, donor stabilized diphosphorus(0) **II**, and diphosphene **III** (Ar* = 2,6-$CHPh_2$-4-*t*BuC_6H_2, NHC^{Dip} = 1,3-(2,6-$iPr_2C_6H_3$)$_2$-imidazole-2-ylidene, R = general monoanionic ligand).

[a]*Tata Institute of Fundamental Research Hyderabad, Gopanpally, Hyderabad-500107, Telangana, India. E-mail: ajana@tifrh.res.in*

[b]*School of Chemical Sciences, National Institute of Science Education and Research, Bhimpur-Padanpur, Jatni, Khurda, Bhubaneswar-752050, Odisha, India*

[c]*Krupp-Chair of General and Inorganic Chemistry, Saarland University, 66123 Saarbrücken, Germany. E-mail: scheschkewitz@mx.uni-saarland.de*

[d]*Department of Medicinal and Aromatic Plants, University of Aksaray, Aksaray, Turkey. E-mail: cemburakyildiz@aksaray.edu.tr*

[e]*Department of Chemistry, Indian Institute of Technology Kanpur, Kanpur-208016, India. E-mail: vc@iitk.ac.in*

† Electronic supplementary information (ESI) available: Thermodynamic data of equilibrium between **1** and **3**, solution and solid state NMR spectra, UV/vis spectra, NMR simulation of compound **6**, X-ray crystallographic data and theoretical details. CCDC 1588456 (**3**), 1588457 (**4**), 1588458 (**5**), 1588459 (**6**) and 1588460 (**7**). For ESI and crystallographic data in CIF or other electronic format see DOI: 10.1039/c8sc00348c

The intriguing difference of reactivity between **I** and **II** and most importantly the fact that reversible coordination of Lewis bases to multiply bonded main group species is limited[7] prompted us to investigate the coordination behaviour of an NHC as an auxiliary base towards a diphosphene **III** as well as the influence on its reactivity. In this context, it may be mentioned that Matsuo and co-workers recently reported the cleavage of the P–P double bond of Rind-substituted diphosphene (Rind = 1,1,3,3,5,5,7,7-octa-R-substituted s-hydrindacen-4-yl) by an NHC to yield two NHC-coordinated phosphinidene fragments. The mechanism was proposed to proceed *via* the formation of an NHC-coordinated, highly polarized diphosphene as a transient intermediate.[15] The coordination of NHC to the heteronuclear and thus naturally polarised P=C bond of phosphaalkenes has been studied by Gates *et al.*[16]

Results and discussion

Since the isolation of the sterically protected diphosphene, Mes*P=PMes* (Mes* = 2,4,6-*t*Bu$_3$-C$_6$H$_2$), by Yoshifuji and co-workers[17] several other diphosphenes have been isolated and characterized.[18] We deliberately chose the relatively unreactive diphosphene Ter^{Mes}P=PTer^{Mes}, **1**[19] and probed its binding with NHC^{Me_4}, **2**.[20] The treatment of **1** with a stoichiometric amount of **2** at room temperature resulted in an immediate colour change from yellow to deep red (Scheme 2). The $^{31}P\{^1H\}$ NMR of the reaction mixture showed two upfield doublets of equal intensity at $\delta = -95.36$ ppm and -0.78 ppm ($^1J_{(P,P)} = 423$ Hz) along with the signal of the free diphosphene **1** at $\delta = 492$ ppm in about 70 : 30 ratio. As this ratio remained unaltered even after 2 h, we suspected that the coordination of NHC might indeed be reversible. The remarkable difference in the chemical shifts accompanied by a large coupling constant proves the presence of two non-equivalent phosphorus nuclei in different electronic environments, which is consistent with the formation of the NHC-diphosphene adduct **3** (Scheme 2).

The single crystal X-ray diffraction analysis of **3** reveals that NHC^{Me_4} is coordinated to one of the P-centres of the former diphosphene moiety (Fig. 1). The P–P bond length in **3** is 2.134(2) Å and thus longer than that observed in **1** (2.029(1) Å),[21] but still substantially shorter than the P–P single bond of diphosphanes, *e.g.* (6-Me-2-pyridyl)(SiMe$_3$)$_2$CPH]$_2$ (2.222(3) Å).[22] The calculated Wiberg Bond Order (WBO) (**1**: 1.812; **3**: 1.116) and the partial NBO charges (**1**: P1 = 0.280, P2 = 0.326; **3**: P1 = 0.494, P2 = −0.116) at the B3LYP/6-311G(d,p) level of theory clearly indicate elongation and polarization of the P=P bond upon coordination of NHC.[23]

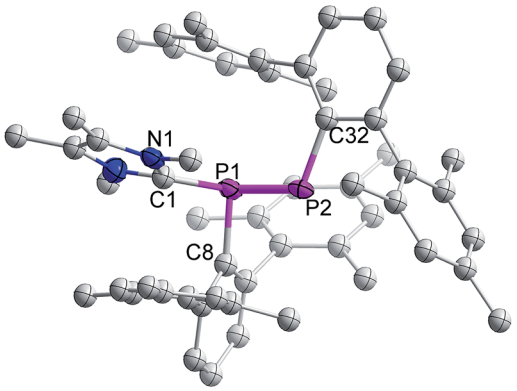

Fig. 1 Molecular structure of **3** (thermal ellipsoids at 50% probability; hydrogen atoms omitted for clarity).

The two nonbonding electron pairs at P2 implied by the ylidic nature of **3** correspond to the HOMO and HOMO−1 (Fig. 2). While the HOMO almost exclusively consists of a p-orbital centered at the formally negatively charged P center, the HOMO−1 and the HOMO−2 are delocalized across the P–P unit and therefore correspond to the s-type lone pairs at the phosphorus centers (Fig. 2). The LUMO is mainly delocalized over the P–C bond between the carbenic carbon and P1.

The carbenic carbon C1 is connected to the P1 center with an angle of 113.26(18)° with respect to the P1–P2 bond vector. The two terphenyl ligands adopt a trans-arrangement with a torsion angle of C8–P1–P2–C32 = 166.8(2)°. The bond distance between the carbenic carbon and coordinated phosphorus of **3** is 1.876(2) Å and hence slightly larger than the corresponding distance in NHC^{Me_4}-coordinated phosphaalkene, MesP=CPh$_2$ (1.8512 Å).[16b]

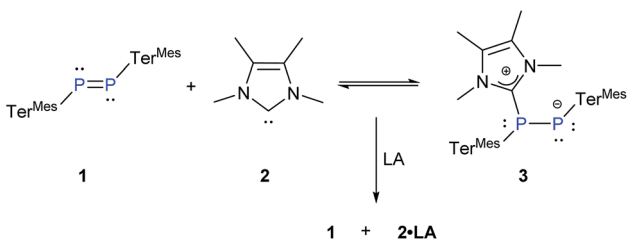

Scheme 2 Reaction of **1** and **2** under the reversible formation of **3** (Ter^{Mes} = 2,6-Mes$_2$C$_6$H$_3$, Mes = 2,4,6-Me$_3$C$_6$H$_2$, LA = Ph$_3$B and ZnCl$_2$).

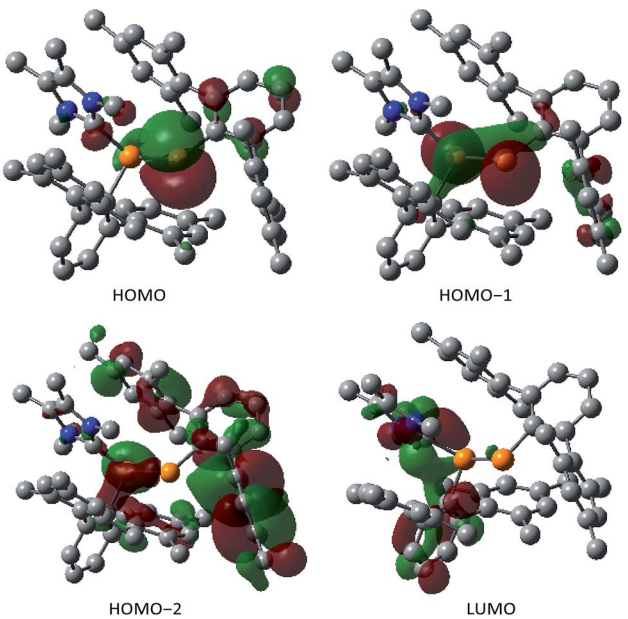

Fig. 2 Frontier molecular orbitals of the compound **3** at 0.04 atomic units.

To substantiate our assertion of reversible coordination of NHC to the P=P moiety, we recorded the $^{31}P\{^1H\}$ NMR of a 1 : 1 mixture of **1** and **2** (0.0805 M solution in toluene-d_8) at variable temperatures (253 to 293 K). Indeed, the proportion of adduct **3** increases at lower temperature as expected on grounds of entropic arguments. We calculated the Gibbs enthalpy of formation of **3** to be $\Delta G_{298} = -11.2 \pm 1.1$ kJ mol^{-1}.[23] In order to check the solvent dependency of the equilibrium, we recorded the solution NMR of a 1 : 1 mixture of **1** and **2** in C_6D_6 and THF-d_8 at room temperature. While diphosphene **1** and NHC-adduct **3** are observed in an almost 3 : 7 ratio along with free NHC^{Me_4} in the comparatively apolar C_6D_6, the more polar THF-d_8 leads to a shift of equilibrium in favour of the polarized adduct **3** (90%). As expected on grounds of the law of mass action, the addition of 2 equivalents of NHC^{Me_4} to **1** shifts the equilibrium almost completely towards the adduct **3**. On the other hand, when equivalent amounts of Lewis acids such as Ph_3B or $ZnCl_2$ are added, NHC^{Me_4} is effectively scavenged and free diphosphene **1** regenerated (Scheme 2). In order to confirm the exclusive presence of **3** in the solid state, we also performed CP-MAS $^{31}P\{^1H\}$ NMR.[23] This reversible addition of NHC^{Me_4}, **2**, to diphosphene, **1**, has similarities with the reactivity of transition metal complexes in terms of ligand exchange.[3]

In order to further substantiate the reversibility of NHC coordination, we monitored the changes in the absorption of **1** (in THF) with increasing concentrations of **2** by UV/vis spectroscopy. A THF solution of free diphosphene **1** absorbs at λ_{max} = 448, 372, and 317 nm. Upon gradual addition of NHC^{Me_4}, **2**, the absorbance at 448 nm increases while the absorbance at 372 nm decreases in intensity as the equilibrium is shifted towards **3**. The absorbance at λ = 317 nm is shifted to λ = 324 nm when the NHC^{Me_4} concentration exceeds more than 1.11 equivalents (1.33, 2.22, and 4.44 equivalents). A clear isosbestic point is revealed at λ = 392 nm (Fig. 3). From the UV/vis studies the Gibbs enthalpy of formation of **3** is estimated to be $\Delta G_{298} = -13.30$ kJ mol^{-1}, which is close to the value obtained from the VT-NMR study ($\Delta G_{298} = -11.2 \pm 1.1$ kJ mol^{-1}).[23]

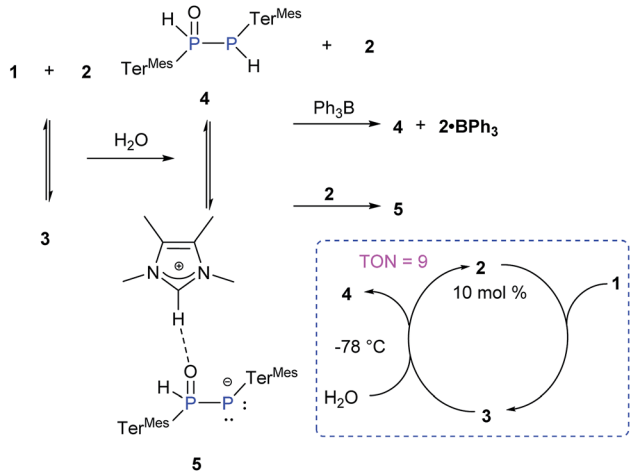

Scheme 3 Reaction of **3** with H_2O (Ter^{Mes} = 2,6-$Mes_2C_6H_3$, Mes = 2,4,6-$Me_3C_6H_2$).

Due to the pronounced polarization of the P=P moiety upon coordination of NHC^{Me_4}, an enhanced reactivity was anticipated. We probed the addition reactions of water and dihydrogen in the presence of NHC^{Me_4} as benchmarks as free diphosphene **1** is inert towards hydrolysis or hydrogenation (Scheme 3). Thus far, only the hydrolysis of Lewis acid-coordinated diphosphene and heteroleptic diphosphenes has been reported.[24]

Addition of one equivalent of H_2O to a THF solution of **3** (1 : 1 mixture of **1** and **2**) at RT led to an immediate colour change from red to yellow (Scheme 3). The presence of four new multiplets in the ^{31}P NMR spectrum with each two of equal intensity at δ = 9.55 and −77.36 ppm and δ = 28.50 and −46.76 ppm indicates complete conversion to two new species.

Indeed, the molecular structure determination reveals the formation of phosphino substituted phosphine oxide **4** (Fig. 4) and phosphido phosphine oxide **5** (Fig. 5) in the course of the reaction (Scheme 3). The solid state structures of these two compounds match well with that of solution state NMR data. The P–P distances involved are 2.1946(8) Å for **4** and 2.1099(11) Å for **5**.

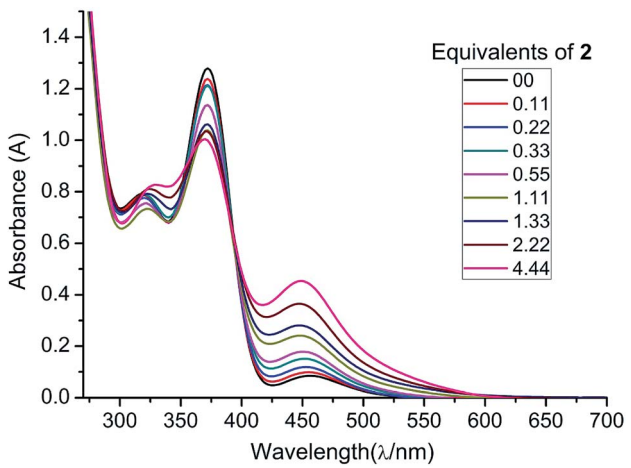

Fig. 3 UV/vis spectra of **1** (black line) in THF with increasing concentrations of **2**.

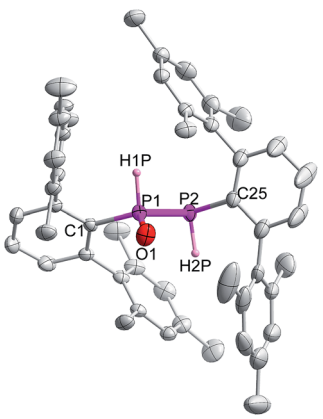

Fig. 4 Molecular structure of **4** at thermal ellipsoids of 50% probability level; all the hydrogen atoms are omitted for clarity except P–H.

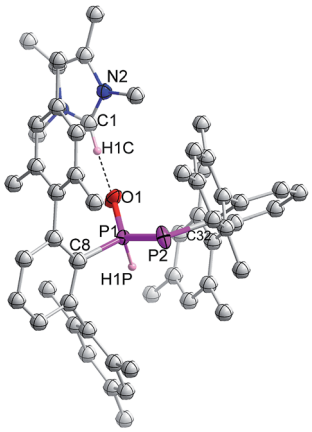

Fig. 5 Molecular structures of **5** at thermal ellipsoids of 50% probability level; all the hydrogen atoms are omitted for clarity except P–H and imidazolium C–H.

These distances are longer than those in **1** or **3** (1 : 1.985(2), 3 : 2.134 Å). The P–O bond length found in **4** is 1.478(2) Å, which is shorter compared with that of **5** (1.492(2) Å) presumably because of a H-bonding interaction with an imidazolium cation.[25] The P–P distance in **4** (2.1946(8) Å) is slightly longer than that observed in the metal carbonyl (Lewis acid) free phospha-Wittig–Horner reagent, (Mes*PH–P(O)(OEt)$_2$) (2.1854 Å).[26]

The Lewis acid free phospha-Wittig–Horner reagent, (Mes*PH-P(O)(OEt)$_2$), is known to be readily deprotonated to the lithiated phospha–Wittig–Horner reagent, Mes*P=P(OLi)(OEt)$_2$.[26] Similarly, the phosphino substituted phosphine oxide **4** is transformed to the corresponding ion pair **5** through deprotonation by NHC^{Me_4}, **2** (Scheme 3). The complete formation of **5** from **4** is observed when 2 equivalents of **2** are added. The ^{31}P NMR spectrum of the phosphino substituted phosphine oxide **4** exhibits two doublets at $\delta = 9.55$ and -77.36 ppm with a $^1J_{P-P}$ of 248 Hz. In **5** the corresponding resonances are observed at $\delta = 28.50$ and -46.76 ppm with a $^1J_{P-P}$ of 464 Hz. These trends are similar to those observed in Mes*PH–P(O)(OEt)$_2$ ($^1J_{P-P}$ = 222 Hz) and Mes*P=P(OLi)(OEt)$_2$ ($^1J_{P-P}$ = 615 Hz).[26] Despite the imidazolium character of the NHC moiety in **5**, the addition of BPh_3 as a NHC scavenger results in the liberation of free **4** as previously observed for standard NHC-coordinated main group species (Scheme 3).[27] The exclusive formation of **4** has also been achieved by the addition of $Et_3N{\cdot}HCl$ to the reaction mixture. In view of the apparent equilibrium, we expected the hydrolysis of **1** to be catalytic in NHC^{Me_4}. In addition, the calculated relative free energy for the formation of **4** from **3** (**3** + H_2O → **4** + **2**) is determined to be $\Delta G_{298} = -12.1$ kcal mol^{-1} at the B3LYP-D3/6311-G(d,p) level of theory.[23] Indeed, treatment of **1** at −78 °C with one equivalent of H_2O in the presence of 10 mol% of **2** leads to >90% of **4** (TON = 9, Scheme 3).[23] At higher temperatures, the hydrolysis of NHC^{Me_4} becomes competitive significantly reducing the yield of **4** and thus the TON.

The reaction of **3** with H_2 does not proceed under ambient conditions. On the other hand, **3** reacts instantaneously with $NH_3{\cdot}BH_3$ as a dihydrogen source affording two diastereomers (***d*/*l*-6** and ***meso*-6**) of dihydrodiphosphane, (Scheme 4). The parent diphosphene **1** only reacts sluggishly with $NH_3{\cdot}BH_3$ taking more than 7 days to afford the product in modest yields.

The ^{31}P NMR spectra of ***d*/*l*-6** and ***meso*-6** exhibit an AA′XX′ pattern with the peaks centered at $\delta = -109.9$ and -101.4 ppm, respectively (Fig. 6). To determine the magnitudes of the coupling constants of the AA′XX′ spin system, a simulation of the ^{1}H and ^{31}P NMR spectra was performed (Fig. 6).[28] Previously, Erickson *et al.* reported the formation of one of the diastereomers of compound **6** by the tin-catalyzed dehydrocoupling of Ter^{Mes}PH$_2$.[29] Based on the current study it can be concluded that the previously reported diastereomer had the *meso* configuration. The initially formed racemic mixture of ***d*/*l*-6** is slowly converted to the *meso*-isomer, ***meso*-6**, reaching equilibrium within 12 h at room temperature. This has been confirmed by performing the reaction and measuring ^{31}P{^{1}H} NMR at −50 °C. DFT calculations at the B3LYP-D3/6-311G(d,p) level of theory indeed show that the ***meso*-6** isomer is lower in free energy than ***d*/*l*-6**, by $\Delta G_{298} = 2.3$ kcal mol^{-1}.[23]

Single crystal X-ray diffraction on crystalline samples of **6** exclusively resulted in a structural model in line with ***meso*-6** (Fig. 7). As this model depends on the somewhat ambiguous determination of the hydrogen positions H1P and H1P*, we cannot exclude the presence of a mixture of isomers in the solid state. Indeed, the CP-MAS ^{31}P{^{1}H} NMR of a crystalline sample shows the presence of both diastereomers.

Finally, to address the complete cleavage of the P–P bond present in **3**, we monitored the 1 : 2 reaction between **1** and **2**. After four days a colour change from deep red to yellow occurred and we observed the appearance of a new ^{31}P resonance at $\delta = -77$ ppm, which is in the range for a carbene-stabilized

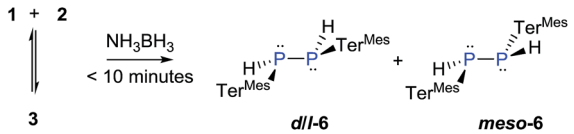

Scheme 4 Reaction of **3** with $NH_3{\cdot}BH_3$ (Ter^{Mes} = 2,6-Mes$_2$C$_6$H$_3$, Mes = 2,4,6-Me$_3$C$_6$H$_2$).

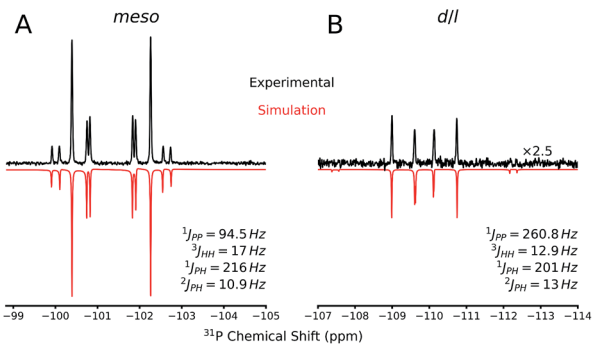

Fig. 6 Comparison between the experimental (black, upper curve) and simulated (red, lower curve) ^{31}P NMR spectrum of (A) ***meso*-6** and (B) ***d*/*l*-6** compounds. The scalar couplings used for the simulations are shown on the lower right side.

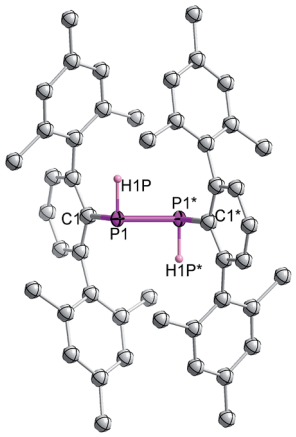

Fig. 7 Molecular structure of *meso*-**6** (thermal ellipsoids of 50% probability level; hydrogen atoms are omitted for clarity).

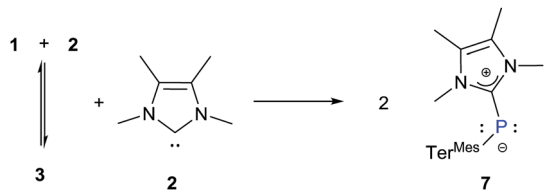

Scheme 5 Reaction of **3** with NHC^{Me_4} (Ter^{Mes} = 2,6-$Mes_2C_6H_3$, Mes = 2,4,6-$Me_3C_6H_2$).

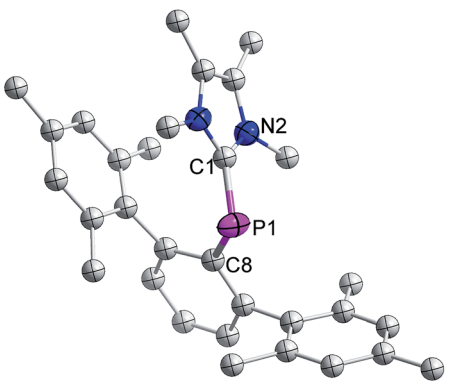

Fig. 8 Molecular structure of **7** at thermal ellipsoids of 50% probability level; all hydrogen atoms are omitted for clarity.

phosphinidene.[30] Subsequently we heated the reaction mixture at 105 °C for 30 h to ensure complete dissociation resulting in the formation of **7** (Scheme 5).

The distance between phosphorus and the carbenic carbon is 1.786(2) Å (Fig. 8), which is comparable with that reported for a NHC-stabilized phosphinidene.[31] However it is shorter than the distance between the phosphorus and carbenic carbon of **3** (1.8306(19) Å).

The formation of **7** from **3** is strong experimental corroboration for the mechanism proposed by Matsuo and co-workers for the cleavage of a P═P bond in a diphosphene.[15]

Conclusions

In summary, we have demonstrated for the first time that the coordination of an N-heterocyclic carbene to a heavier double bond results in a striking reactivity enhancement. The reversible coordination of the NHC to a diphosphene significantly enhances the reaction rate of hydrolysis and hydrogenation by the ammonia–borane complex. In the case of hydrolysis, we have demonstrated that the reaction is catalytic in NHC.

Experimental

General

All experiments were carried out under an argon atmosphere using standard Schlenk techniques or in a PL-HE-2GB Innovative Technology GloveBox. *n*-Hexane, diethyl ether, THF, and toluene were dried using a PS-MD-5 Innovative Technology solvent purification system. Benzene was refluxed over sodium/benzophenone, and then distilled and stored under argon. Starting compounds $Ter^{Mes}_2P_2$, **1**[19] and NHC^{Me_4}, **2**[20] were prepared according to known literature procedures. Benzene-d_6 was dried and distilled over potassium under argon. NMR spectra were recorded with a Bruker NanoBay 300 MHz NMR machine. ^{1}H and ^{13}C{^{1}H} NMR spectra were referenced to the peaks of residual protons of the deuterated solvent (^{1}H) or the deuterated solvent itself (^{13}C{^{1}H}). Solid-state ^{31}P{^{1}H} NMR spectra were obtained on a Bruker Avance 400 MHz spectrometer with a wide-bore magnet and operating at 400.13 MHz (^{1}H) and 163.32 MHz (^{31}P). Powdered samples were packed in a 4 mm o.d. zirconia rotor. The diameter of the Probe is 89 mm with a spinning speed of 13 KHz. The ^{31}P{^{1}H} CP MAS experiment was performed using a ^{1}H 90° pulse of 3.3 μs, with a contact time of 5 ms, CPD Spinal64 as the decoupling scheme, and a recycle delay of 3 s. UV/vis spectra were acquired using a Jasco V-670 spectrometer using quartz cells with a path length of 0.1 cm. Elemental analyses were performed on a Leco CHN-900 analyzer. Melting points were determined in closed NMR tubes under an argon atmosphere and are uncorrected.

Synthesis of 3

10 mL of THF is added to a Schlenk flask containing **1** (0.357 g, 0.518 mmol) and **2** (0.084 g, 0.673 mmol) at room temperature. After stirring for about 5 minutes, all volatiles are removed under vacuum. The resulting residue is extracted with 10 mL of *n*-pentane (2 times) and the combined filtrate is kept at −30 °C overnight resulting in the formation of bright red crystals, yield: 0.211 g (51.9%). In solution compound **3** is in equilibrium with **1** and **2**. NMR data from a 1 : 1 stoichiometric ratio of **1** and **2** in C_6D_6 at RT (almost 30% of **1** and **2** and 70% of **3**): mp: 185 °C (decomposed). ^{1}H NMR (300 MHz, C_6D_6, 298 K): δ = 1.25 (s, 3H, C–CH_3 of NHC^{Me_4}), 1.30 (s, 3H, C–CH_3 of NHC^{Me_4}), 1.57 (s, 2H, C–CH_3 of **2**), 1.89 (br, 14H, 6H from CH_3 of Mes and remaining 8H from CH_3 of Mes of **1**), 2.17 (s, 18H, CH_3 of Mes), 2.21 (s, 16H, 12H from CH_3 of Mes and remaining 4H from CH_3 of Mes of **1**), 2.66 (s, 3H, N–CH_3 of NHC^{Me_4}), 3.35 (br, 5H, 3H from N–CH_3 and 2H from N–CH_3 of **2**), 6.53 (s, br, 2H, Ar–*H*), 6.62–6.67 (m, 4H, Ar–*H*), and 6.78–7.04 (m

13H, 8H from Ar–*H* and 5H from Ar–*H* of **1**) ppm. NMR data from a 1 : 2 stoichiometric ratio of **1** and **2** in C_6D_6 at RT to get unambiguous 1H NMR data of **3**. ^{1}H NMR (300 MHz, C_6D_6, 298 K): δ = 1.28 (s, 3H, C–CH_3 of NHC^{Me_4}), 1.33 (s, 3H, C–CH_3 of NHC^{Me_4}), 1.82 (br, 6H, CH_3 of Mes), 2.16 (s, 18H, CH_3 of Mes), 2.21 (s, 12H, CH_3 of Mes), 2.66 (s, 3H, N–CH_3 of NHC^{Me_4}), 3.36 (s, br, 3H, N–CH_3 of NHC^{Me_4} and 6H, N–CH_3 of **2**), 6.52 (s, br, 2H, Ar–*H*), 6.62–6.66 (m, 4H, Ar–*H*), 6.78 (s, br, 4H, Ar–*H*), and 6.86–7.04 (m, 4H, Ar–*H*) ppm. ^{13}C{^{1}H} NMR (75.43 MHz, C_6D_6, 298 K): δ = 7.73 (1C, C–*C*H$_3$ of NHC^{Me_4}), 8.29 (1C, C–*C*H$_3$ of NHC^{Me_4}), 21.07 (3C, *C*H$_3$ of Mes), 21.37 (4C, *C*H$_3$ of Mes), 21.92 (3C, *C*H$_3$ of Mes), 22.66 (1C, *C*H$_3$ of Mes), 22.88 (1C, *C*H$_3$ of Mes), 30.46 (1C, d, $^3J_{(P,C)}$ = 26.85 Hz, N–*C*H$_3$ of NHC^{Me_4}), 32.83 (1C, d, $^3J_{(P,C)}$ = 19.39 Hz, N–*C*H$_3$ of NHC^{Me_4}), 120.00 (1C, Ar–*C*H), 123.04 (1C, CH$_3$–*C* of NHC^{Me_4}), 125.82 (1C, CH$_3$–*C* of NHC^{Me_4}), 126.89 (1C, Ar–*C*H), 127.31 (2C, Ar–*C*H), 127.63 (2C, Ar–*C*H), 127.98 (2C, Ar–*C*H), 128.29 (1C, Ar–*C*H), 128.58 (3C, Ar–*C*H), 130.46 (1C, Ar–*C*H), 130.51 (1C, Ar–*C*H), 133.77 (2C, Ar–C_{quat}), 135.55 (2C, Ar–C_{quat}), 135.70 (3C, Ar–C_{quat}), 137.46 (2C, Ar–C_{quat}), 138.22 (1C, Ar–C_{quat}), 138.40 (1C, Ar–C_{quat}), 138.78 (2C, Ar–C_{quat}), 140.95 (2C, Ar–C_{quat}), 142.78 (1C, Ar–C_{quat}), 142.84 (2C, Ar–C_{quat}), 146.93 (1C, Ar–C_{quat}), 147.18 (1C, Ar–C_{quat}), 150.17 (1C, Ar–C_{quat}), 150.28 (1C, N*C*N), 151.83 (1C, d, $^1J_{(C,P)}$ = 9.50 Hz, Ar–C_{quat}), and 152.33 (1C, Ar–C_{quat}) ppm. ^{31}P NMR (121.5 MHz, C_6D_6, 298 K): δ = −95.36 (d, $^1J_{(P,P)}$ = 423 Hz) and −0.78 (d, $^1J_{(P,P)}$ = 423 Hz) ppm. CP-MAS ^{31}P{^{1}H} NMR (163.32 MHz, 298 K): δ = −99.07 (d, $^1J_{(p,p)}$ = 430 Hz, 1P) and 3.99 (d, $^1J_{(p,p)}$ = 430 Hz, 1P) ppm. UV/vis (*n*-hexane): IR (KBr, cm^{-1}): $\bar{\nu}$ = 405 (s), 414 (vs), 422 (s), 435 (w), 449 (vs), 474 (vw), 489 (vw), 501 (vw), 530 (m), 548 (vw), 576 (m), 588 (m), 657 (vw), 669 (m), 712 (s) 738 (br, s), 768 (w), 788 (s), 802 (s), 846 (vs), 872 (vw), 907 (br, vw), 998 (vw), 1030 (s), 1080 (w), 1107 (w), 1178 (m), 1239 (w), 1363 (m), 1439 (m), 1569 (w), 1607 (w), 1652 (w), and 2356 (w).

Reaction of 3 with BPh_3

In a glovebox, **1** (0.020 g, 0.029 mmol) and **2** (0.0047 g, 0.037 mmol) were dissolved in THF (0.2 mL) in an NMR tube. After about 5 minutes BPh_3 (0.0091 g, 0.037 mmol, in 0.2 mL THF) was added resulting in an instant colour change from red to yellow. Subsequent addition of 0.1 mL C_6D_6 allowed for the recording of a ^{31}P NMR spectrum, which revealed the complete conversion of **2** into **1**.

Synthesis of 2·BPh_3

Inside the glovebox, 0.019 g (0.08 mmol) of BPh_3 was weighed into an NMR tube. A benzene-d_6 solution of 0.010 g (0.08 mmol, in 0.5 mL C_6D_6) of **1** was added at room temperature. ^{1}H NMR measurements confirm the formation of **2·BPh$_3$**. ^{1}H NMR (300 MHz, C_6D_6, 298 K): δ = 1.11 (s, 6H, CH_3C–CCH_3), 2.63 (s, 6H, NCH_3), 7.18–7.27 (m, 3H, Ar–*H*), 7.34 (t, $^3J_{(H,H)}$ = 7.40 Hz, 6H, Ar*H*), and 7.68 (d, $^3J_{(H,H)}$ = 6.95 Hz, 6H, Ar*H*) ppm.

Reaction of 3 with $ZnCl_2$

Inside the glovebox, **1** (0.024 g, 0.035 mmol) and **2** (0.0056 g, 0.045 mmol) were dissolved in THF (0.2 mL) in an NMR tube. After about 5 minutes $ZnCl_2$ (0.0061 g, 0.045 mmol, in 0.2 mL THF) was added leading to an instant colour change from red to yellow. After addition of 0.1 mL C_6D_6, a ^{31}P NMR spectrum was recorded showing complete conversion of **2** into **1**.

Synthesis of 4

In a 50 mL Schlenk flask, 0.392 g (0.57 mmol) of compound **1** and 0.080 g (0.64 mmol) of **2** were dissolved in 15 mL of THF. The reaction mixture was stirred for 10 minutes. Subsequently, degassed water (12 μL, 0.65 mmol) was added at room temperature and allowed to stir for 1.5 h. The red colour of the solution slowly transformed into orange. This reaction mixture was then added into a THF (5 mL) suspension of $Et_3N{\cdot}HCl$ (0.094 g, 0.68 mmol) and allowed to stir for 30 minutes resulting in the gradual fading of the colour. All volatiles were then evaporated and extracted with hot *n*-hexane (15 mL). Incipient crystallization happened at room temperature. Isolated yield 0.310 g (78%). Mp: >190 °C. ^{1}H NMR (300 MHz, C_6D_6, 298 K): δ = 1.79 (s, 6H, CH_3 of Mes), 1.93 (s, 6H, CH_3 of Mes), 2.05 (s, 6H, CH_3 of Mes), 2.28 (s, 6H, CH_3 of Mes), 2.31 (s, 12H, CH_3 of Mes), 3.21 (ddd, $^1J_{(P,H)}$ = 248.70 Hz, $^2J_{(H,P)}$ = 13.34 Hz, $^3J_{(H,H)}$ = 8.10 Hz, 1H, HP(O)–P–*H*), 7.19 (ddd, $^1J_{(P,H)}$ = 473.31 Hz, $^2J_{(H,P)}$ = 32.35 Hz, $^3J_{(H,H)}$ = 8.10 Hz, 1H, *H*–P(O)–P*H*), 6.70–6.74 (m, 4H, Ar–*H*), 6.77 (br, 1H, Ar–*H*), 6.79–6.81 (m, 3H, Ar–*H*), 6.87 (s, 4*H*, Ar–*H*), and 6.96–7.07 (m, 2H, Ar–*H*) ppm. ^{13}C{^{1}H} NMR (75.43 MHz, C_6D_6, 298 K): δ = 21.03 (2C, *C*H$_3$ of Mes), 21.37 (2C, *C*H$_3$ of Mes), 21.63 (1C, *C*H$_3$ of Mes), 21.72 (6C, *C*H$_3$ of Mes), 21.79 (1C, *C*H$_3$ of Mes), 129.01 (2C, Ar–*C*H), 129.04 (2C, Ar–*C*H), 129.14 (2C, Ar–*C*H), 129.36 (2C, Ar–*C*H), 129.47 (1C, Ar–*C*H), 129.87 (1C, Ar–*C*H), 129.98 (3C, Ar–*C*H), 132.58 (d, $^4J_{(C,P)}$ = 2.27Hz, 1C, Ar–*C*H), 133.42 (d, $^1J_{(P,C)}$ = 4.52 Hz, 1C, Ar–C_{quat}), 134.51 (d, $^1J_{(P,C)}$ = 4.52 Hz, 1C, Ar–C_{quat}), 136.74 (2C, Ar–C_{quat}), 136.75 (2C, Ar–C_{quat}), 136.77 (2C, Ar–C_{quat}), 137.93 (1C, Ar–C_{quat}), 139.50 (2C, Ar–C_{quat}), 145.70 (1C, Ar–C_{quat}), 145.83 (1C, Ar–C_{quat}), 147.58 (d, 1C, $J_{(C,P)}$ = 5.28 Hz), and 147.73 (d, 1C, $J_{(C,P)}$ = 4.52 Hz) ppm. ^{31}P NMR (121.5 MHz, C_6D_6, 298 K): δ = 9.55 (ddd, $^1J_{(P,P)}$ = 248.70 Hz, $^1J_{(P,H)}$ = 473.31 Hz, $^2J_{(H,P)}$ = 13.34 Hz, H*P*(O)–PH) and −77.36 (dt, $^1J_{(P,P)}$ = $^1J_{(P,H)}$ = 248.70 Hz, $^2J_{(H,P)}$ = 32.35 Hz, Ter-*P*-H) ppm. ^{31}P{^{1}H} NMR (121.5 MHz, C_6D_6, 298 K): δ = 9.55 (d, $^1J_{(P,P)}$ = 248.70 Hz, H*P*(O)–PH) and −77.36 (d, $^1J_{(P,P)}$ = 248.70 Hz, Ter-*P*-H) ppm. CP-MAS ^{31}P{^{1}H} NMR (163.32 MHz, 298 K): δ = 9.64 (d, $^1J_{(p,p)}$ = 230 Hz, H*P*(O)–PH) and −78.48 (d, $^1J_{(p,p)}$ = 230 Hz, Ter-*P*-H) ppm. IR (KBr, cm^{-1}): $\bar{\nu}$ = 1131 (s), 1187 (s), 1232 (s), 1307 (w), 1370 (m), 1412 (w), 1431 (m), 1450 (m), 1466 (w), 1482 (w), 1501 (m), 1513 (w), 1534 (s), 1553 (s), 1564 (m), 1605 (m), 1633 (w), 1677 (m), 1691 (m), 1712 (m), 1726 (m), 1764 (w), 1785 (w), 1820 (w), 1841 (w), 1862 (w), 1886 (w), 1500 (w), 1555 (s), 1570 (m), 1610 (m), 1641 (m), 1676 (m) 1711 (m), 1727 (m), 2313 (m, P–H), 2352 (s, P–H), 2727 (m), and 2849 (w). Elemental analysis: calcd for $C_{48}H_{52}OP_2$ (706.87): C, 81.56; H, 7.41. Found: C, 80.81; H, 7.17.

Synthesis of 5

In a 50 mL Schlenk flask, 0.510 g (0.740 mmol) of compound **1** and 0.120 g (0.960 mmol) of **2** were dissolved in 15 mL of THF. Water (17.4 μL, 0.960 mmol) was added at room temperature and allowed to stir for 1.5 h. The red colour of the solution slowly transformed into orange. The reaction mixture was then

evaporated and extracted with hot toluene (20 mL). Crystallization occurred upon cooling at room temperature. Isolated yield 0.530 g (86.13%). Mp: >190 °C (decomposed) and at 175 °C the color changed slowly towards white. ^{1}H NMR (300 MHz, THF-d_8, 298 K): δ = 1.80 (s, 6H, 6H, CH_3 of Mes), 1.81 (s, 6H, CH_3 of Mes), 1.92 (s, 6H, C–CH_3 of NHC^{Me_4}), 2.00 (s, 6H, CH_3 of Mes), 2.18 (s, 12H, CH_3 of Mes), 2.22 (s, 6H, CH_3 of Mes), 3.51 (s, 6H, N–CH_3 of NHC^{Me_4}), 6.32 (s, 1H, Ar–*H*), 6.34 (s, 1H, Ar–*H*), 6.44 (s, 2H, Ar–*H*), 6.47 (s, 2H, Ar–*H*), 6.50–6.54 (m, 3H, Ar–*H*), 6.57 (s, 3H, Ar–*H*), 6.74 (s, 2H, Ar–*H*), 7.08 (t, 1H, $^{3}J_{(H,H)}$ = 7.60 Hz, Ar–*H*), 6.96 (d, 1H, $^{1}J_{(P,H)}$ = 464.15 Hz, P–*H*), and 10.65 (s, br, 1H, N–C*H*–N of NHC^{Me_4}) ppm. ^{13}C{^{1}H} NMR (75.43 MHz, C_6D_6, 298 K): δ = 7.66 (2C, C–*C*H$_3$ of NHC^{Me_4}), 21.02 (1C, *C*H$_3$ of Mes), 21.05 (1C, *C*H$_3$ of Mes), 21.34 (2C, *C*H$_3$ of Mes), 21.44 (2C, *C*H$_3$ of Mes), 21.58 (1C, *C*H$_3$ of Mes), 21.61 (1C, *C*H$_3$ of Mes), 22.14 (1C, *C*H$_3$ of Mes), 22.32 (1C, *C*H$_3$ of Mes), 22.47 (1C, *C*H$_3$ of Mes), 22.55 (1C, *C*H$_3$ of Mes), 33.42 (2C, CH$_3$–*C* of NHC^{Me_4}), 119.82 (2C, Ar–*C*H), 126.31 (2C, 4,5-*C* of NHC^{Me_4}), 127.56 (3C, Ar–*C*H), 128.04 (2C, Ar–*C*H), 128.18 (2C, Ar–*C*H), 128.37 (2C, Ar–*C*H), 128.52 (1C, Ar–*C*H), 129.63 (1C, Ar–*C*H), 129.72 (1C, Ar–*C*H), 134.42 (2C, Ar–C_{quat}), 134.90 (2C, Ar–C_{quat}), 136.66 (2C, Ar–C_{quat}), 137.26 (2C, Ar–C_{quat}), 137.56 (2C, Ar–C_{quat}), 137.87 (2C, Ar–C_{quat}), 141.51 (1C, Ar–C_{quat}), 141.55 (1C, Ar–C_{quat}), 142.90 (1C, Ar–C_{quat}), 142.95 (1C, Ar–C_{quat}), 143.04 (1C, Ar–C_{quat}), 143.08 (1C, Ar–C_{quat}), 143.25 (1C, Ar–C_{quat}), 144.63 (1C, Ar–C_{quat}), 144.65 (1C, Ar–C_{quat}), 144.72 (1C, Ar–C_{quat}), and 144.76 (1C, N*C*N) ppm. ^{31}P NMR (121.5 MHz, C_6D_6, 298 K): δ = 28.50 (*t*, 1P, $^{1}J_{(P,P)}$ = $^{1}J_{(P,H)}$ 464.15Hz, P–*P*–O) and −46.76 (*d*, 1P, $^{1}J_{(P,P)}$ = 464.15 Hz, *P*–P–O) ppm. ^{31}P{^{1}H} NMR (121.5 MHz, C_6D_6, 298 K): δ = 28.50 (d, $^{1}J_{(P,P)}$ = 464.15 Hz, P–*P*–O) and −46.76 (*d*, $^{1}J_{(P,P)}$ = 464.15 Hz, *P*–P–O) ppm. CP-MAS ^{31}P{^{1}H} NMR (163.32 MHz, 298 K): δ = 27.04 (d, $^{1}J_{(p,p)}$ = 465 Hz, P–*P*–O) and −47.00 (*d*, $^{1}J_{(P,P)}$ = 465 Hz, *P*–P–O) ppm. UV/vis (THF): $\lambda_{max}(\varepsilon)$ = 330 (5244), 390 (9754), and 445 (4410) nm (L mol^{-1} cm^{-1}). IR (KBr, cm^{-1}): $\bar{\nu}$ = 750 (s), 844 (s), 907 (s), 988 (vs), 1157 (w), 1216 (w), 1270 (w), 1369 (m), 1426 (vw), 1444 (w), 1466 (m), 1485 (m), 1548 (m), 1563 (w), 1582 (w), 1642 (s), 1657 (s), 1688 (s), 1707 (m), 1723 (s), 1754 (m), 1779 (m), 1809 (vw), 1838 (s), 1857 (s), 1879 (m), 1900 (m), 1926 (w), 1951 (w), 1979 (w), 2352 (m P–H), 2380 (m, P–H), and 2921 (br). Elemental analysis: calcd for $C_{55}H_{64}N_2OP_2$ (831.06): C, 79.49; H, 7.76; N, 3.37. Found: C, 79.60; H, 7.89; N, 3.73.

Catalytic hydrolysis of 1

0.277 g (0.402 mmol) of **1** and 0.005 g (0.0402 mmol) of **2** were dissolved in about 10 mL of THF (10 mL) and cooled down to −78 °C. Subsequently, 8 μL (0.45 mmol) of water was added and the reaction mixture was allowed to warm to room temperature. Subsequent ^{31}P{^{1}H} NMR measurements show the formation of **4** in about 95% spectroscopic yield.

Synthesis of 6

In a 50 mL Schlenk flask, 0.334 g (0.49 mmol) of compound **1** and 0.080 g (0.64 mmol) of **2** were dissolved in 15 mL of THF. The reaction mixture was stirred for 10 minutes. Afterwards, 10 mL of a THF solution of $NH_3 \cdot BH_3$ (0.020 g, 0.64 mmol) was added at room temperature. The reaction mixture was allowed to stir for 30 minutes during which the red colour of the solution slowly faded to colourless. ^{31}P NMR showed complete formation of compound **6** as *d*/*l* and *meso* isomers. All volatiles were evaporated and the residue was extracted with hot *n*-hexane (15 mL). Crystallization occurred at room temperature, and a second crop was obtained at −20 °C. Isolated yield 0.300 g (89%). Mp: >190 °C. ^{1}H NMR of the *meso* isomer (300 MHz, C_6D_6, 298 K): δ = 1.90 (s, 12H, CH_3 of Mes), 2.05 (s, 12H, CH_3 of Mes), 2.28 (s, 12H, CH_3 of Mes), 3.02 (centre of the AA′XX′ multiplet pattern, 2H, P*H*–P*H*, fitted with $^{1}J_{(31P,31P)}$ = 94.5 Hz, $^{3}J_{(1H,1H)}$ = 17.0 Hz, $^{1}J_{(31P,1H)}$ = 216 Hz, and $^{2}J_{(31P,1H)}$ = 10.9 Hz), 6.74 (s, 2H, Ar–*H*), 6.76 (s, 2H, Ar–*H*), 6.81 (s, 4H, Ar–*H*), 6.83 (s, 4H, Ar–*H*), and 6.98 (t, $^{3}J_{(H,H)}$ = 7.41, 2H, Ar–*H*) ppm. Selected ^{1}H NMR of the *d*/*l* isomer (300 MHz, C_6D_6, 298 K): δ = 1.91 (s, 12H), 1.96 (s, 12H), 2.30 (s, 12H), and 4.01 (centre of the AA′XX′ multiplet pattern, 2H, P*H*–P*H*, fitted with $^{1}J_{(31P,31P)}$ = 260.8 Hz, $^{3}J_{(1H,1H)}$ = 12.9 Hz, $^{1}J_{(31P,1H)}$ = 201 Hz, and $^{2}J_{(31P,1H)}$ = 13 Hz) ppm. ^{13}C{^{1}H} NMR (75.43 MHz, C_6D_6, 298 K): δ = 21.35 (1C, *C*H$_3$ of Mes), 21.38 (2C, *C*H$_3$ of Mes), 21.41 (1C, *C*H$_3$ of Mes), 21.48 (1C, *C*H$_3$ of Mes), 21.55 (2C, *C*H$_3$ of Mes), 21.61 (1C, *C*H$_3$ of Mes), 21.71 (4C, *C*H$_3$ of Mes), 128.69 (2C, Ar–*C*H), 128.79 (2C, Ar–*C*H), 128.92 (2C, Ar–*C*H), 129.08 (2C, Ar–*C*H), 129.02 (2C, Ar–*C*H), 129.12 (2C, Ar–*C*H), 129.37 (2C, Ar–*C*H), 134.14 (1C, Ar–C_{quat}), 134.27 (1C, Ar–C_{quat}), 134.41 (1C, Ar–C_{quat}), 136.12 (1C, Ar–C_{quat}), 136.36 (3C, Ar–C_{quat}), 136.54 (1C, Ar–C_{quat}), 136.65 (3C, Ar–C_{quat}), 136.76 (3C, Ar–C_{quat}), 139.88 (3C, Ar–C_{quat}), 140.05 (1C, Ar–C_{quat}), 140.70 (1C, Ar–C_{quat}), 146.78 (2C, Ar–C_{quat}), and 146.87 (1C, Ar–C_{quat}) ppm. ^{31}P NMR (121.5 MHz, C_6D_6, 298 K): δ = −101.4 (*meso* isomer, centre of the AA′XX′ pattern as seen in the ^{1}H decoupled spectrum; non-decoupled spectrum fit with $^{1}J_{(31P,31P)}$ = 94.5 Hz, $^{3}J_{(1H,1H)}$ = 17.0 Hz, $^{1}J_{(31P,1H)}$ = 216 Hz, and $^{2}J_{(31P,1H)}$ = 10.9 Hz (the same as that for the corresponding ^{1}H spectrum)) and −109.9 (*d*/*l* isomer, centre of the AA′XX′ pattern as seen in the ^{1}H decoupled spectrum; non-decoupled spectrum fit using $^{1}J_{(31P,31P)}$ = 260.8 Hz, $^{3}J_{(1H,31H)}$ = 12.9 Hz, $^{1}J_{(31P,1H)}$ = 201 Hz, and $^{2}J_{(31P,1H)}$ = 13 Hz (the same as that for the corresponding ^{1}H NMR spectrum)) ppm. ^{31}P{^{1}H} NMR (121.5 MHz, C_6D_6, 298 K): δ = −101.38 (s, *meso* isomer) and −109.9 (s, *d*/*l* Isomer) ppm. CP-MAS ^{31}P{^{1}H} NMR (163.32 MHz, 298 K)): δ = −101.38 (s, *meso* isomer) and − 104.13 (s, *d*/*l* isomer) ppm. IR (KBr, cm^{-1}): $\bar{\nu}$ =: 845 (s), 1398 (w), 1432 (w), 1457 (w), 1485 (w), 1567 (s), 1610 (s), 1647 (vw), 1726 (m), 1757 (vw), 1804 (vw), 1866 (m), 1932 (m), 2325 (s, P–H), 2403 (vw, P–H), 2727 (s), 2855 (w), and 2907 (w). Elemental analysis: calcd for $C_{48}H_{52}P_2$ (690.87): C, 83.45; H, 7.59. Found: C, 82.56; H, 7.27.

Synthesis of 7

In a 25 mL Schlenk flask 0.202 g (0.293 mmol) of compound **1** and 0.072 g (0.586 mmol) of **2** were dissolved in 10 mL of toluene. The red reaction mixture was heated at 105 °C for 30 h. During the course of the reaction, the color of the reaction mixture changed from red to yellow. After 12 h at 0 °C yellow crystals of **7** were obtained. The resulting mother liquor was concentrated to 5 mL and kept at −20 °C. After one day a second crop of crystals was collected. Total yield: 0.225 g (81.8%). Single

crystals suitable for X-ray diffraction analysis were obtained from a saturated solution of toluene at 0 °C after one day. Mp: >200 °C. ^{1}H NMR (300 MHz, C_6D_6, 298 K): $\delta = 1.25$ (s, 6H, C–CH_3 of NHC^{Me_4}), 2.17 (6H, *p*-CH_3 of Mes), 2.40 (12H, *o*-CH_3 of Mes), 2.84 (s, 6H, N–CH_3 of NHC^{Me_4}), 6.78 (4H, Ar–*H*), and 6.99–7.08 (m, 3H Ar–*H*) ppm. ^{13}C{^{1}H} NMR (75.43 MHz, C_6D_6, 298 K): $\delta =$ 8.83 (2C, C–CH_3 of NHC^{Me_4}), 21.51 (4C, CH_3 of Mes), 21.56 (2C, CH_3 of Mes), 34.12 (N–CH_3 of NHC^{Me_4}), 34.24 (N–CH_3 of NHC^{Me_4}), 122.50 (1C, Ar–*C*H), 122.55 (2C, CH_3–*C* of NHC^{Me_4}), 128.53 (4C, Ar–*C*H), 128.98 (2C, d, $J_{(C,P)} = 1.38$, Ar–*C*H), 134.37 (1C, Ar–C_{quat}), 136.26 (1C, Ar–C_{quat}), 142.78 (1C, Ar–C_{quat}), 142.82 (1C, Ar–C_{quat}), 144.68 (1C, Ar–C_{quat}), 144.86 (1C, Ar–C_{quat}), 150.67 (1C, Ar–C_{quat}), 151.42 (1C, Ar–C_{quat}), 167.40 (1C, Ar–C_{quat}), and 168.70 (1C, Ar–C_{quat}) ppm. ^{31}P NMR (121.5 MHz, C_6D_6, 298 K): $\delta = -77$ ppm. CP-MAS ^{31}P{^{1}H} NMR (163.32 MHz, 298 K): $\delta = -77.05$ ppm. UV/vis (*n*-hexane): $\lambda_{max}(\varepsilon) =$ 446 (11 244), 382 (5375), and 310 (2553) nm (L mol^{-1} cm^{-1}). IR (KBr, cm^{-1}): $\bar{\nu} =$ 408 (s), 420 (vs), 432 (s), 465 (vs), 552 (s), 583 (m), 593 (vs), 658 (m), 677 (s), 720 (m), 745 (s), 775 (m), 797 (s), 856 (vs), 879 (s), 907 (s), 1042 (br, vs), 1085 (m), 1107 (m), 1185 (w), 1234 (w), 1660 (m), 1705 (m), 1856 (m), 1876 (w), 2346 (br, w), and 2372 (w). Elemental analysis: calcd for $C_{31}H_{37}N_2P$ (468.62): C, 79.45; H, 7.96; N, 5.98. Found: C, 79.24; H, 8.02; N, 6.06.

Conflicts of interest

There are no conflicts to declare.

Acknowledgements

This work is supported by the Tata Institute of Fundamental Research Hyderabad, Gopanpally, Hyderabad-500107, Telangana, India, SERB-DST (EMR/2014/001237), India, Research Group Linkage Programme of Alexander von Humboldt Foundation, Germany, and Saarland University, Germany. VC is thankful to the Department of Science and Technology, New Delhi, India, for a National J. C. Bose fellowship. We thank the reviewers for their comments to improve the manuscript.

Notes and references

1 (*a*) J. A. Osborn, F. H. Jardine, J. F. Young and G. Wilkinson, *J. Chem. Soc. A*, 1966, 1711–1732; (*b*) P. Meakin, J. P. Jesson and C. A. Tolman, *J. Am. Chem. Soc.*, 1972, **94**, 3240–3242; (*c*) S. K. Tanielyan, R. L. Augustine, N. Marin and G. Alvez, *ACS Catal.*, 2011, **1**, 159–169.

2 (*a*) N. H. Park, E. V. Vinogradova, D. S. Surry and S. L. Buchwald, *Angew. Chem., Int. Ed.*, 2015, **54**, 8259–8262; (*b*) P. L. Arrechea and S. L. Buchwald, *J. Am. Chem. Soc.*, 2016, **138**, 12486–12493; (*c*) D. A. Culkin and J. F. Hartwig, *Organometallics*, 2004, **23**, 3398–3416; (*d*) B. Su, T.-G. Zhou, X. W. Li, X. R. Shao, P. L. Xu, W. L. Wu, J. F. Hartwig and Z. J. Shi, *Angew. Chem., Int. Ed.*, 2017, **56**, 1092–1096; (*e*) X. Jiang, J. J. Beiger and J. F. Hartwig, *J. Am. Chem. Soc.*, 2017, **139**, 87–90.

3 P. P. Power, *Nature*, 2010, **463**, 171–177.

4 G. C. Welch, R. R. S. Juan, J. D. Masuda and D. W. Stephan, *Science*, 2006, **314**, 1124–1126.

5 Y. Peng, B. D. Ellis, X. Wang, J. C. Fettinger and P. P. Power, *Science*, 2009, **325**, 1668–1670.

6 F. Buß, P. Mehlmann, C. Mück-Lichtenfeld, K. Bergander and F. Dielmann, *J. Am. Chem. Soc.*, 2016, **138**, 1840–1843.

7 (*a*) K. Leszczyńska, K. Abersfelder, A. Mix, B. Neumann, H. G. Stammler, M. J. Cowley, P. Jutzi and D. Scheschkewitz, *Angew. Chem. Int. Ed.*, 2012, **51**, 6785–6788; (*b*) M. J. Cowley, V. Huch, H. Rzepa and D. Scheschkewitz, *Nature Chem.*, 2013, **5**, 876–879.

8 A. F. Eichhorn, S. Fuchs, M. Flock, T. B. Marder and U. Radius, *Angew. Chem., Int. Ed.*, 2017, **56**, 10209–10213.

9 (*a*) G. H. Spikes, J. C. Fettinger and P. P. Power, *J. Am. Chem. Soc.*, 2005, **127**, 12232; (*b*) G. D. Frey, V. Lavallo, B. Donnadieu, W. W. Schoeller and G. Bertrand, *Science*, 2007, **316**, 439–441.

10 (*a*) A. Jana, M. Majumdar, V. Huch, M. Zimmer and D. Scheschkewitz, *Dalton Trans.*, 2014, **43**, 5175–5181; (*b*) A. Jana, I. Omlor, V. Huch, H. S. Rzepa and D. Scheschkewitz, *Angew. Chem., Int. Ed.*, 2014, **53**, 9953–9956.

11 (*a*) L. Liu, D. A. Ruiz, D. Munz and G. Bertrand, *Chem*, 2016, **1**, 147–153; (*b*) M. M. Hansmann, R. Jazzar and G. Bertrand, *J. Am. Chem. Soc.*, 2016, **138**, 8356–8359.

12 M. M. Hansmann and G. Bertrand, *J. Am. Chem. Soc.*, 2016, **138**, 15885–15888.

13 Y. Wang, Y. Xie, P. Wei, R. B. King, H. F. Schaefer III, P. v. R. Schleyer and G. H. Robinson, *J. Am. Chem. Soc.*, 2008, **130**, 14970–14971.

14 D. Dhara, D. Mandal, A. Maiti, C. B. Yildiz, P. Kalita, N. Chrysochos, C. Schulzke, V. Chandrasekhar and A. Jana, *Dalton Trans.*, 2016, **45**, 19290–19298.

15 N. Hayakawa, K. Sadamori, S. Tsujimoto, M. Hatanaka, T. Wakabayashi and T. Matsuo, *Angew. Chem., Int. Ed.*, 2017, **56**, 5765–5769.

16 (*a*) J. I. Bates, P. Kennepohl and D. P. Gates, *Angew. Chem. Int. Ed.*, 2009, **48**, 9844–9847; (*b*) P. K. Majhi, K. C. F. Chow, T. H. H. Hsieh, E. G. Bowes, G. Schnakenburg, P. Kennepohl, R. Streubel and Derek P. Gates, *Chem. Commun.*, 2016, **52**, 998–1001.

17 M. Yoshifuji, I. Shima, N. Inamoto, K. Hirotsu and T. Higuchi, *J. Am. Chem. Soc.*, 1981, **103**, 4587–4589.

18 M. Yoshifuji, *Eur. J. Inorg. Chem.*, 2016, 607–615.

19 E. Urnéžius and J. D. Protasiewicz, *Main Group Chem.*, 1996, **1**, 369–372.

20 N. Kuhn and T. Kratz, *Synthesis*, 1993, 561–562.

21 J. D. Protasiewicz, M. P. Washington, V. B. Gudimetla, J. L. Payton and M. C. Simpson, *Inorg. Chim. Acta*, 2010, **364**, 39–45.

22 P. C. Andrews, S. J. King, C. L. Raston and B. A. Roberts, *Chem. Commun.*, 1998, 547–548.

23 See the ESI† for the details.

24 (*a*) J. Borm, G. Huttner, O. Orama and L. Zsolnai, *J. Organomet. Chem.*, 1985, **282**, 53–67; (*b*) N. Nagahora, T. Sasamori, N. Takeda and N. Tokitoh, *Chem.–Eur. J.*, 2004, **10**, 6146–6151; (*c*) C. Moser, F. Belaj and

R. Pietschnig, *Chem.–Eur. J.*, 2009, **15**, 12589–12591; (*d*) L. Weber, S. Buchwald, A. Rühlicke, H. G. Stammler and B. Neumann, *Z. Anorg. Allg. Chem.*, 1993, **619**, 934–942.

25 D. Mandal, B. Santra, P. Kalita, N. Chrysochos, A. Malakar, R. S. Narayanan, S. Biswas, C. Schulzke, V. Chandrasekhar and A. Jana, *ChemistrySelect*, 2017, **2**, 8898–8910.

26 K. Esfandiarfard, A. I. Arkhypchuk, A. Orthaber and S. Ott, *Dalton Trans.*, 2016, **45**, 2201–2207.

27 (*a*) A. Jana, V. Huch, H. S. Rzepa and D. Scheschkewitz, *Angew. Chem., Int. Ed.*, 2015, **54**, 289–292; (*b*) H. Cui, J. Zhang and C. Cui, *Organometallics*, 2013, **32**, 1–4.

28 Z. Tošner, R. Andersen, B. Stevensson, M. Edén, N. C. Nielsena and T. Vosegaard, *J. Magn. Reson.*, 2014, **246**, 79–93.

29 K. A. Erickson, L. S. H. Dixon, D. S. Wright and R. Waterman, *Inorg. Chim. Acta*, 2014, **422**, 141–145.

30 O. Back, M. H. Ellinger, C. D. Martin, D. Martin and G. Bertrand, *Angew. Chem., Int. Ed.*, 2013, **52**, 2939–2943.

31 T. Krachko, M. Bispinghoff, A. M. Tondreau, D. Stein, M. Baker, A. Ehlers, J. C. Slootweg and H. Grützmacher, *Angew. Chem., Int. Ed.*, 2017, **56**, 7948–7951.